



## RESEARCH ARTICLE

### STRUCTURAL AND PHOTOLUMINESCENCE PROPERTY OF CDO AND ZN DOPED CDO NANOPOWDERS SYNTHESISED BY SOLUTION COMBUSTION METHOD

\*Yesudoss, T.

Department of Physics, Annai Vailankannai Arts and Science College, Thanjavur-07

#### ARTICLE INFO

##### Article History:

Received 02<sup>nd</sup> March, 2017  
Received in revised form  
24<sup>th</sup> April, 2017  
Accepted 10<sup>th</sup> May, 2017  
Published online 30<sup>th</sup> June, 2017

##### Keywords:

CdO,  
Solution Combustion,  
Structural,  
Optical.

#### ABSTRACT

CdO/CdOZn nanoparticles were synthesised by Solution Combustion method. The synthesized particles were characterized by x-ray diffraction, ultraviolet-visible spectroscopy, field emission scanning electron microscopy, photoluminescence spectroscopy and inductively coupled plasma measurements. X-ray diffraction studies indicate that the obtained CdO/CdOZn have a cubic structure at nanoscale. The band gaps were calculated from the absorption peak of ultraviolet-visible spectrum and it was found to vary from 2.47 - 2.28 eV on Zn doping. Increase in transmittance upon Zn doping was observed. Field emission scanning electron microscopy images showed that the synthesized samples composed of nanoparticles with the average diameter of 20.8 – 34.7 nm.

Copyright©2017, Yesudoss. This is an open access article distributed under the Creative Commons Attribution License, which permits unrestricted use, distribution and reproduction in any medium, provided the original work is properly cited.

#### INTRODUCTION

In recent years, synthesis and characterization of binary chalcogenides of II–VI group semiconductor materials in nanometer scale has been a rapidly growing area of research, due to their exceptional chemical and physical properties that are different from those of either bulk material or single atom (1,2). Nanomaterials of conducting oxides like cadmium oxide (CdO), zinc oxide (ZnO), tin dioxide (SnO<sub>2</sub>), indium oxide (In<sub>2</sub>O<sub>3</sub>) and titanium oxide (TiO<sub>2</sub>) have attracted the deliberation of researchers over the last two decades by reason of their outstanding applications in solar cells, flat panel displays, photovoltaic devices, smart windows and optical transmission devices. Of the above mentioned conducting oxides, CdO is the first reported transparent *n*-type semiconducting oxide (TCO). Eventhough it was first reported conducting oxide; it has not been widely studied as much of other oxide material like SnO<sub>2</sub>, ZnO and In<sub>2</sub>O<sub>3</sub>, owing to its relatively small energy gap 2.2–2.7 eV with a direct band gap and 1.36–1.98 eV with indirect band gap (3). This low band gap results the low optical conductivity in short wave length region.

As a result, the physical properties of CdO could be improved for optoelectronic applications by doping with indium (In), tin(Sn), aluminium(Al), scandium, zinc (Zn) and yttrium (Y) which tunes its *n*-type conductivity and increases the band gap. Moreover, CdO nanoparticles are mainly used in photovoltaic cells, solar cells, phototransistors, IR reflectors, transparent electrodes, gas sensors and in variety of other materials. As it has high reflectance in the infrared region, together with high transparency (above 70 %) in the visible region, it is also used as heat mirrors. Nanocrystalline CdO not only has unique optical and opto-electrical characteristics but it also has catalytic properties that make the compound suitable for use in the photo-degradation of toxic organic compounds, dyes, pigments and other environmental pollutants (Tadjarodi *et al.*, 2014). A variety of nanostructures has been reported in CdO, which include nanoparticles (Yufanyi, 2014), nano clusters (Srinivasaraghavana *et al.*, 2013), nanowires, nanorods (Li *et al.*, 2013), nanobelts (Pan, 2001), nanocubes (Tadjarodi, 2011), and rhombus-like Nanostructure (Ashoka, 2010). All these nanostructures are being synthesized by several techniques. Ashoka *et.al.* (2010), and Barve *et.al.* followed a facile hydrothermal process with a post-reaction calcination to prepare the nanomaterials. Biological synthesis of CdO nanoparticles, using flower broth of *A. wilhelmsii* has been demonstrated by Karimi *et al.*, (2013). Likewise Kalpanadevi *et al.*, (2013) succeeded in the preparation of CdO nanostructures from the low temperature thermal

\*Corresponding author: Yesudoss, T.,

Department of Physics, Annai Vailankannai Arts and Science College, Thanjavur-07.

decomposition of inorganic precursors whereas sol-gel method has been proposed by de Anda Reyesa *et al.* (2012). A well known solvothermal method has been followed by Ghosh *et al.* (2004) have obtained the CdO nanoparticles by the decomposition of the cupferron complex in the presence of tri-n-octylphosphine oxide (TOPO). A simple and rapid microwave - assisted combustion method was developed to synthesize CdO nanospheres by Selvam *et al.* (2011). This valuable information motivated us to work in CdO nanostructures. There are a number of articles discuss the synthesis of CdO nanoparticles, nanowires and nanofilms by chemical co-precipitation method (Waghulade, 2007; Barve, 2014). Preparation of CdO nanoparticles using cadmium acetate and ammonia solution has been reported in Ref.no (20). We have chosen the Solution Combustion method here for the synthesis of CdO nanostructures, in view of the fact that an extensive literature review infers that this method is good for the synthesis of metal oxide nanoparticles. Because it is a low cost process, and easy to control the particle size. In our previous work (Pushpanathan *et al.*, 2012), we confirmed that precipitation method gives the smaller nanoparticle with good optical properties, in comparison with other synthesis procedure such as sol-gel synthesis, hydrothermal reaction and electrochemical routes. Hence, here we have opted for the Solution Combustion method. For the above mentioned applications of CdO nanoparticles, we were interested in this work in the optical and antibacterial properties of CdO nanoparticles as a function of Zn composition.

## EXPERIMENTAL PROCEDURE

### MATERIALS AND METHOD

Analytical grade cadmium nitrate ( $\text{Cd}(\text{NO}_3)_2 \cdot 2\text{H}_2\text{O}$ ), zinc nitrate ( $\text{Zn}(\text{NO}_3)_2 \cdot 2\text{H}_2\text{O}$ ) and Urea supplied by Merck were used to synthesize undoped CdO and Zn doped CdO nanoparticles. All these chemicals were used without further refinement. The beaker and other glass wares used in this work were washed with acid. Ethanol and double distilled water were used as solvent for sample preparation. The detailed synthesis process was as follows

#### Synthesis of CdO and Zn doped CdO nanoparticles

CdO and two different concentration of Zn doped CdO nanoparticles were efficiently synthesized by solution combustion method using the above mentioned chemicals. Three samples were synthesized for the present study. The mechanism for the growth of CdO nanoparticles from cadmium nitrate precursor can be explained as follows. Initially, cadmium nitrate precursor is first dissolved in water and Urea is also added further to it with calculated ratio. The above mentioned metal nitrates and Urea in stoichiometric ratios were completely dissolved in distilled water. The fuel-to-oxidant ratio was derived from the total oxidizing and reducing valences of the oxidizer and fuel using concepts of propellant chemistry. The mixture was heated in a Pyrex beaker on a Muffle furnace which was preheated to 450°C. The viscous resin was bubbled up, the excess of free water evaporated and it was auto ignited with the rapid evolution of large volume of gasses. The ignition persisted for less than a minute, leaving behind a residual brown colour fine powder. For the synthesis of  $\text{Cd}_{0.97}\text{Zn}_{0.03}\text{O}$  and  $\text{Cd}_{0.94}\text{Zn}_{0.06}\text{O}$  samples, appropriate amount

of cadmium nitrate and zinc nitrate were dissolved in mixture of water along with Urea under the same experimental procedure.

### Characterization

The crystalline structure of the samples was analyzed by X-ray diffraction (XRD) using a Bruker AXSD8 Advance instrument equipped with Ni filtered  $\text{CuK}\alpha$  radiation ( $\lambda = 1.54187 \text{ \AA}$ ) in the range of 10-80° in steps of 0.0025 at a scan speed of 2°/min with scanning rate of 1°/min operated at 40 kV/30 mA. The morphology of the synthesized powder was examined by FE-SEM (JEOL – JSM – 6301 FE-SEM) operated at an accelerating voltage, above 5 kV/20 mA and a magnification of  $5 \times 10^4$ . An inductively coupled plasma atomic emission spectrometer (ICP-AES; Varian Vista Pro, CCD Simultaneous, Springvale, Australia) was used for the determination of the Zn and Cd content of the nanopowders. To identify the functional groups and to confirm the presence Cd ions, the samples were examined with Fourier Transform Infrared Spectrometer Shimadzu-8400S spectrometer (Shimadzu Corporation, Kyoto, Japan) at a resolution of  $2 \text{ cm}^{-1}$ . The measurements were carried out in the region 400 – 4000  $\text{cm}^{-1}$  using KBr as the beam splitter. Optical absorption and transmission spectra were recorded using Shimadzu-UV-2550-8030 (Shimadzu Corporation, Kyoto, Japan) UV-Vis spectrophotometer with a slit width of 5 nm and a light source change wavelength of 360 nm, at room temperature in the range of 190 to 800 nm. For this study, the nanopowders were dispersed in deionized water and mixed well. Finally, Photoluminescence (PL) response of the powder samples was carried out by means PL spectrometer (Kimon, SPEC-14031K, Japan) with a He-Cd laser source. A line spectrum of 350 nm has been used to excite the samples.

## RESULTS AND DISCUSSION

### Structural characterization

The XRD patterns of CdO and Zn doped CdO nanoparticles are shown in Figure 1. The diffraction peaks with  $2\theta = 33.2, 38.5, 55.4, 65.9,$  and  $70.4^\circ$  correspond to the crystal plans of (111), (200), (220), (311) and (222) of single phase CdO face-centered cubic phase, respectively. However, the diffraction peaks are slightly shifted to higher angles. The high intensity peaks (111) and (200) have been used to estimate the average crystalline size of sample with the help of Scherer equation  $D = 0.89\lambda / \beta \cos\theta$ , where  $\lambda$ , is the wavelength of the  $\text{CuK}\alpha$  radiation (0.154056 nm), and  $\theta$  is the peak position and  $\beta$  is the Full Width at Half Maximum (FWHM). The average crystallite size found to be ~21 nm, ~31 nm, and ~35 nm for CdO,  $\text{Cd}_{0.97}\text{Zn}_{0.03}\text{O}$  and  $\text{Cd}_{0.94}\text{Zn}_{0.06}\text{O}$  samples. Also the sharpness of XRD peaks indicates that particles are in crystalline nature. Further, no indication of secondary phases such as  $\text{CdO}_2$ ,  $\text{Cd}(\text{OH})_2$ , and  $\text{CdCO}_3$  are detected in the XRD pattern, indicating the formation of CdO crystalline phase. It can be seen that the crystal size increases from about 21 nm (CdO) to 33 nm for ( $\text{Cd}_{0.94}\text{Zn}_{0.06}\text{O}$ ). This is directly related to the crystallization of nanoparticle. The lattice constant ( $a$ ) and volume of the unit cell ( $V$ ) calculated from the XRD data using the following equation.  $a = \sqrt{3} d_{(111)}$ ,  $V = a^3 \text{ nm}^3$ , respectively. Since (111) peak has the highest intensity in the cases, this peak was considered for the lattice constant calculation also.

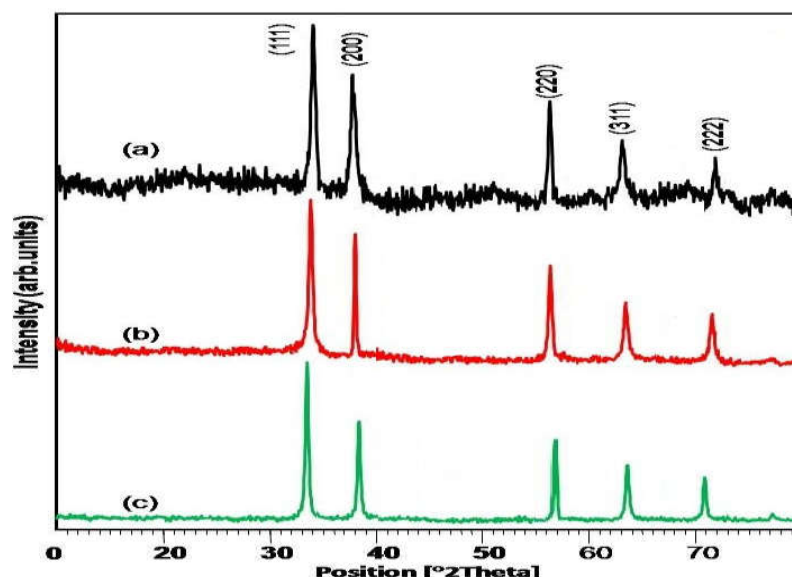


Figure 1. XRD (a) undoped CdO, (b)  $\text{Cd}_{0.97}\text{Zn}_{0.03}\text{O}$ , (c)  $\text{Cd}_{0.94}\text{Zn}_{0.06}\text{O}$

Table 1. Lattice constant, unit cell volume undoped and Zn doped CdO nanoparticles

Sample	(hkl) value	Grain size 'D' (nm)	Average grain size	Interplaner distance (d) (Å)	Lattice constant 'a' (Å)	Unit cell volume 'V' (Å) <sup>3</sup>
CdO	111	20.8	20.8	2.7121	4.697	103.62
	200	20.7		2.3476	4.695	103.49
$\text{Cd}_{0.97}\text{Zn}_{0.03}\text{O}$	111	29.9	30.5	2.7086	4.693	103.34
	200	31.2		2.3468	4.690	103.16
$\text{Cd}_{0.94}\text{Zn}_{0.06}\text{O}$	111	32.9	34.7	2.7134	4.698	103.69
	200	36.5		2.3471	4.693	103.34

Therefore, the lattice constant of CdO and Zn doped CdO was refined and found to be  $a = \sim 4.676$  (2)Å, 4.679(5), and 4.6868(5) Å, respectively, which is lower than bulk CdO (4.695Å) it matches well with the standard data for CdO nanoparticles reported in JCPDS Data Card No. (75–0594). Volume of the unit cell ( $V = a^3$ ) is  $\sim 103 \text{ \AA}^3$ . Further, the XRD profile shows that CdO nanoparticles are strongly crystallized with a preferred (111) orientation, which has been observed in previous work (22-24).

#### UV-Vis Spectrum Analysis

Figure 2(a-c) shows the optical absorption versus wavelength of the CdO and Zn doped CdO nano powders. It is seen from these figures that the undoped CdO exhibits maximum absorption ( $\lambda_{max}$ ) at 503 nm. A progressive red shift from 510 nm to 545 nm has been recorded as the Zn concentration increases from 3 (wt%) to 6 (wt%). This is attributed to the quantum size effect. The corresponding energy gap ( $E_g$ ) for the reported three samples has been calculated using the equation

$$E_g = \frac{1240 \text{ eV}}{\lambda_{max}}$$

Where,  $h$  is Planck's constant ( $6.626 \times 10^{-34} \text{ Js}$ ),  $c$  is the velocity of light, and  $\lambda_{max}$  is the excitonic absorption edge. The energy gap calculated to be 2.46, 2.43, and 2.28eV for the samples of CdO,  $\text{Cd}_{0.97}\text{Zn}_{0.03}\text{O}$  and  $\text{Cd}_{0.94}\text{Zn}_{0.06}\text{O}$  samples, respectively. It can be seen that the band gap linearly decreases from 2.46 to 2.28 eV on doping. Helen and co-workers also found to decrease in energy gap of CdO with Zn doping (Helen *et al.*, 2014).

Therefore, UV-Vis spectrum analysis reveals that Zn doping decreases the energy gap of CdO nanoparticles. Table 1 shows the relation between Zn concentration, lattice parameter, grain size; unit cell volume and energy gap of the synthesized samples and their pictorial representation is given in figure 3. Undoped CdO shows the very low transmittance of 15% in the visible and near-IR region (530-1100 nm). It can be observed that the CdO nanoparticles doped with 3% of Zn shows the moderate transmittance of 30%. Furthermore, 6% Zn doping increased the transmittance maximum to 80%. This behaviour shows that Zn dopant enhances the optical transmittance of CdO. The transmittance graph presented here confirms that Zn doping in CdO matrix improves the transmittance by  $\sim 65\%$ . As limited articles are available on CdO:Zn nanoparticles, we unable to compare our result with others work.

#### Microstructure and Composition Analysis

The FESEM micrographs of synthesized nanopowders of  $\text{Cd}_{1-x}\text{Zn}_x\text{O}$  ( $x = 0.00, 0.03, \text{ and } 0.06$ ) are shown in figure 5 (a-c). The undoped CdO sample has nanoparticles of spherical shape. It can be seen that some nanoparticles combined together and formed agglomeration. It should be noted that there is no voids. Particle size of undoped CdO is estimated to be about 13 nm and uniformly distributed throughout the entire surface. (See figure 5(a)). The influence of Zn on CdO nanoparticles are clearly seen in the FESEM images of the doped samples. Due to doping of 3(wt%) Zn, the morphology is changed from nanoparticle to rock like structure which is composed of nanoparticles and nano-rods.

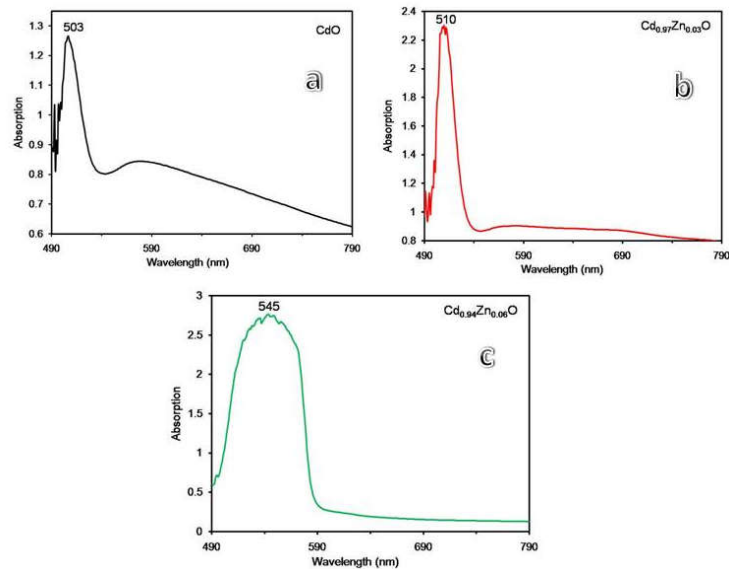


Figure 2(a-c) shows the optical absorption versus wavelength of the CdO and Zn doped CdO nano powders

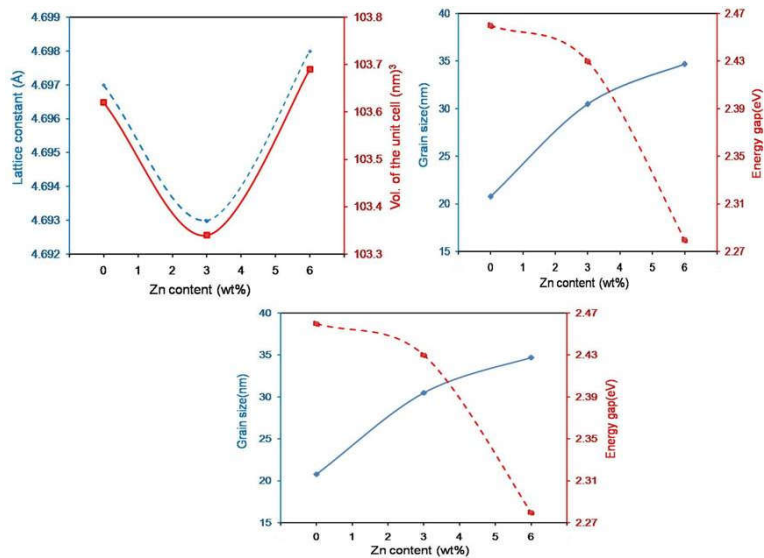


Figure 3: The relation between Zn concentration, lattice parameter, grain size; unit cell volume and energy gap of the synthesized samples

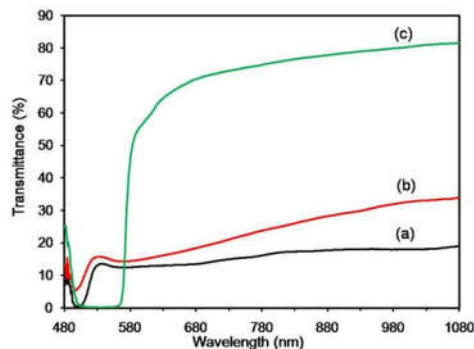


Figure 4. Transmittance spectrum of the synthesized CdO and CdZnO nanoparticles

The interesting thing is that the addition of Zn ion cumulates many nanoparticles in a particular region there by creating the rock-like structure. This accumulation of particles in a particular region creates voids between the grains. In some other regions, these small size nano-rods aligned themselves in the same direction which is highlighted in a box.

Particle size also increased to 24 nm. This increase in particle size with Zn doping may be the fact of build up of some of doped Zn at crystallite boundaries which then enhances accumulation and fusion of crystallites forming larger grains and thus increases the particle size in comparison to the undoped CdO (Refer Fig 5b).

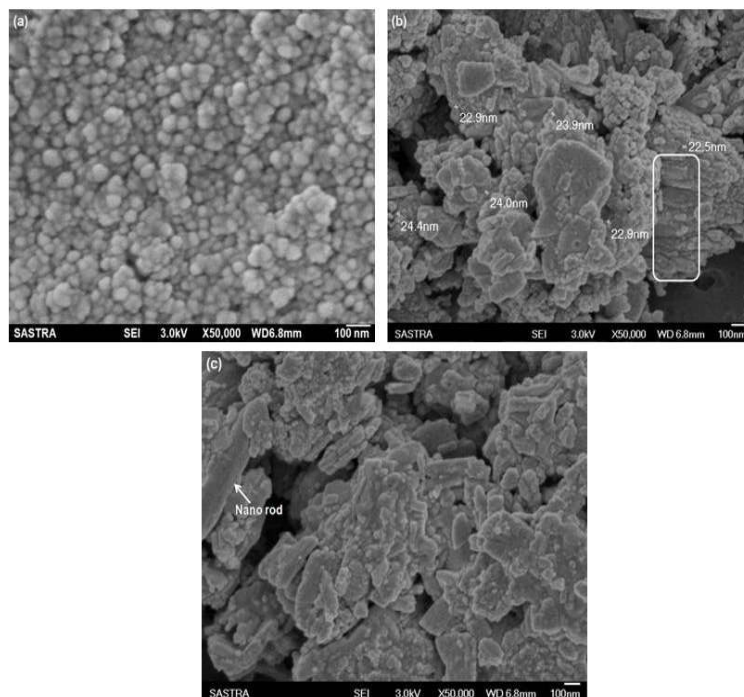


Figure 5: FESEM micrographs of synthesized nanopowders of  $Cd_{1-x}Zn_xO$  ( $x = 0.00, 0.03, \text{ and } 0.06$ )

**Table 2. Result of composition analysis of the synthesized Zn doped CdO samples studied by ICP – AES**

Composition used for sample preparation	ICP -AES		Composition based on ICP – AES analysis
	Cd (wt %)	Zn (wt %)	
$Cd_{0.97}Zn_{0.03}O$	96.2	2.8	$Cd_{0.962}Zn_{0.028}O$
$Cd_{0.94}Zn_{0.06}O$	93.4	5.6	$Cd_{0.934}Zn_{0.056}O$

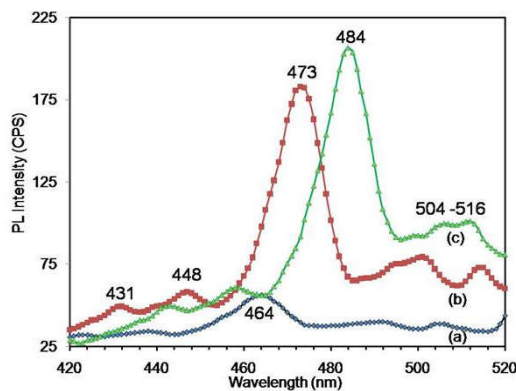


Figure 6. Room temperature PL spectrum of the synthesized nanoparticles

**Table 3. IR peaks and their assignments for prepared CdO:Zn nanoparticles**

Assignments	Wavenumber ( $cm^{-1}$ )		
	CdO	$Cd_{0.97}Zn_{0.03}O$	$Cd_{0.94}Zn_{0.06}O$
Asymmetrical stretching of $H_2O$ molecules	3605	3604	3603
Symmetrical stretching of $H_2O$ molecules	3410	3421	3411
C-H asymmetrical stretching vibrations	2923	2924	2924
C-H symmetrical stretching vibrations	1076	1075	1076
Absorption of $CO_2$ molecule from the air	2471	2471	2472
C=O stretching vibrations	1794	1796	1794
C-O stretching vibrations	1387	1410	1409
Cd-Zn-O bond	-	858- 719	858- 719
Cd -O bond	460	448	457

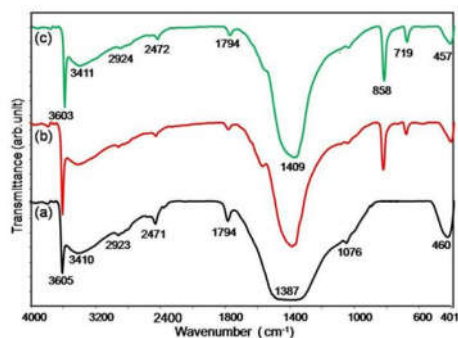


Figure 7. FTIR spectrum of the synthesized nanoparticles (a) undoped CdO, (b) Cd<sub>0.97</sub>Zn<sub>0.03</sub>O, (c) Cd<sub>0.94</sub>Zn<sub>0.06</sub>O nanoparticles.

In particular, we observed a dramatic change in microstructure from nanoplates to nano rods as the dopant concentration is further increased to 6 (wt%). This further increase in Zn ions results in increase in the size of the rock-like structure. Moreover, a large size nano-rod of nearly 800 nm length and 200 nm width can be seen in the 6(wt%) Zn doping (Fig 5c). We believed that this microstructural transformation could be attributed to the extremely small dimensions of the nanoparticles with high surface energy. Therefore, the FESEM analysis infers that Zn ions cumulates the CdO nanoparticles and creates the nano rods. The rod-like CdO nano structure is useful for gas sensing application, which is going on. The analysis of the chemical composition by analytical quantitative technique like the ICP-AES is important because it establishes exactly how much Zn can be incorporated into CdO. We already confirmed that for metal dopant ICP analysis more effective than energy-dispersive x-ray spectroscopy (EDS) analysis. For that reason, composition of Zn doped CdO has been determined by ICP-AE analysis, which shows that the percentage of zinc in the prepared powder samples is nearly close to the concentration of Zn taken for synthesis (Table 2)

### Photoluminescence (PL) Study

Figure 6 shows the PL spectra of the CdO and Zn doped CdO nanoparticles calcinated at 400°C recorded at room temperature. The PL spectrum displays three emission peaks. The less intensity peak appears at 431- 448 nm (2.87 – 2.77 eV) indicates the violet emission, 464 -484 nm (2.67 – 2.56 eV) indicates the blue emission and the peak between 504-516 nm (2.46 – 2.40 eV) corresponds the orange emission. The less intense violet emission peak is attributed to the transition from conduction band to the deep holes trapped levels *i.e.*, Cadmium vacancies ( $V_{Cd}$ ). The samples show two types of blue band they are blue band I (464 nm) and blue band II (484 nm). The blue band I is the result of cadmium intrinsic vacancy ( $Cd_i$ ) and the intensity of this peak depends on the  $Cd_i$ . Blue band II at 484 nm can be ascribed to the direct recombination of conduction electron in the conduction band ( $Cd_{3d}$ ) and a hole in the valance band ( $O_{2p}$ ). Typical orange emission observed at 504-512 nm is from the positively charged single ion oxygen vacancy present on the surface of the nanoparticles. From PL study, it is clear that Zn doping favours for the violet emission in CdO nanoparticles. It has been reported that bulk CdO didn't show luminescence emission (26). But we observed weak luminescence behaviour for undoped CdO nanoparticle; it may be due to quantum size effect. As the Zn concentration increases, the intensity of violet emission increases and the peak shifted from 464 nm to 484 nm.

It is the fact that the increasing Zn ion concentration decreases the number of defect sites which results in increase in intensity of the emission.

### Fourier Transform Infrared Spectroscopy Study

Figure 7 depicts the FT-IR spectrum of the resulting nanopowders after heating treatment at 400 °C for 4h. The absorption bands that appeared evidently belong to the organic functional groups of the synthesized nanopowders. The absorption bands at 3605 cm<sup>-1</sup> and 3410 cm<sup>-1</sup> can be attributed to the asymmetrical and symmetrical stretching vibration bands of H<sub>2</sub>O molecules, respectively. The observed vibration mode at 2923 cm<sup>-1</sup> and 1076 cm<sup>-1</sup> can be assigned to the C-H asymmetrical and symmetrical stretching vibrations, respectively. The peak centred at 2472 cm<sup>-1</sup> belongs to the absorption of CO<sub>2</sub> molecule from the air at the time of sample preparation. The specified weak peak at 1794 cm<sup>-1</sup> and broad peak at 1387 cm<sup>-1</sup> are assigned to C=O and C-O stretching vibrations of the carbonyl groups, respectively. Peaks below 1000 cm<sup>-1</sup> is useful in understanding the metal oxide bonding. In this sense, the strong narrow absorption bands at 719 cm<sup>-1</sup> represents the Cd-Zn-O bond exists in Zn doped samples and a weak peak at 485 cm<sup>-1</sup> represents the Cd-O phase (27). It is interesting to note that incorporation of Zn atom decreased the broadness of the region between 1612 cm<sup>-1</sup> 1409 cm<sup>-1</sup>, which implies that Zn concentration limits the vibration of carbonyl groups. Shift in the peak from 457 cm<sup>-1</sup> to 460 cm<sup>-1</sup> confirms the Zn dopant in the CdO nanocrystals. Likewise, Zn concentration also increased the intensity of absorption peak at 719 cm<sup>-1</sup>. IT peak assignments are given in table 3. Therefore, the FTIR spectra confirmed the presence of Zn with the evidence of 858 cm<sup>-1</sup>, 719 cm<sup>-1</sup> in the prepared samples.

### Conclusion

In conclusion, we have successfully synthesized the CdO and Zn doped CdO nanocrystals were synthesized by simple chemical precipitation method. XRD analysis confirms that the samples contain the nanosize particles. The energy gap calculation from UV-Vis analysis confirms that the prepared nanoparticles possesses indirect band gap and also it infers that Zn doping increases the band gap of CdO. The FESEM images of CdO clearly revealed that it has sphere-like structure of uniform nanoparticles with an average size of 29 nm. The morphology of the Zn doped CdO powder nano-rod and rock-like structure with the average size of 35 nm. We conclude that Zn doping align the CdO these nanoparticles in a particular direction and form the rock-like and nano-rod like morphology. Compositional analysis and FTIR analysis confirmed the presence of Zn in CdO matrix. PL analysis confirms that the Zn incorporation shift the emission of CdO from blue band I to blue band II.

### REFERENCES

- Ashoka, S., Chithaiah, P., Chandrappa, G.T. 2010. Studies on the synthesis of CdCO<sub>3</sub> nanowires and porous CdO powder, *Materials Letters* 64 173–176,  
 Barve, A.K., Gadegone, S.M., Lanjewar, M.R. and Lanjewar, R.B. 2014. *International Journal of Engineering Research and Applications*, 35-38.

- Barve, A.K., Gadegone, S.M., Lanjewar, M.R. and Lanjewar, R.B. Synthesis and Characterization of CdO Nanomaterial and their Photocatalytic Activity, *International Journal on Recent and Innovation Trends in Computing and Communication*, 2 2806 – 2810.
- Bhosale, C.H., Kambale, A.V., Kokate, K.Y. 2005. Structural, optical and electrical properties of chemically sprayed CdO thin films, *Mater.Sci. Eng. B*. 122, 67-71.
- Ejhieh, A.N. and Banan, Z. 2011. A comparison between the efficiency of CdS: A and CdO/zeolite A as catalysts in photodecolorization of crystal violet. *Desalination*. 279. 146-151.
- Ghosh, M., Rao, C.N.R. 2004. Solvothermal synthesis of CdO and CuO nanocrystals, *Chemical Physics Letters* 393 493–497.
- Helen, S.J., Suganthi, D., Mahalingam, T. 2014. Effect of Zinc Doping on CdO Thin Films Prepared by Spray Pyrolysis Technique, National Conference on Advanced Technology Oriented Materials (ATOM-2014), 8-9<sup>th</sup> Dec-.
- Hutt, L. 2013. A book on review of near infrared reflectance properties of metal oxide nanostructures, JANUARY, Publisher: GNS Science, ISBN: 9781972192849.
- Jefferson, P.H., Hatfield, S.A., Veal, T.D., King, P.D.C. Mc Connville, C.F., Perez, J.Z. and Sanjose, V.M. 2008. Bandgap and effective, mass of epitaxial cadmium oxide. *Appl. Phys. Lett.* 92 022101.
- Kalpanadevi, K., Sinduja, C. R. and Manimekalai, R. 2013. *ISRN Inorganic Chemistry*, Volume, Article ID 823040, 5 pages.
- Karimi Andeani, J., Mohsenzadeh, S. 2013. Phytosynthesis of Cadmium Oxide Nanoparticles from Achillea Wilhelmsii Flowers, *Journal of Chemistry*, Article ID 147613, 4 pages.
- A.K.Barve, S.M.Gadegone, M.R. Lanjewar and R.B.Lanjewar, Synthesis and Characterization of CdO Nanomaterial and their Photocatalytic Activity, *International Journal on Recent and Innovation Trends in Computing and Communication*, 2 , 2806 – 2810.
- Kim, J. H., Hong, Y. C., Uhm, H. S. 2007. Direct Synthesis and Characterization of CdO Nano-Cubes, *Japanese Journal of Applied Physics*, 46 7A.
- Li, W., Li, M., Xie, S., Zhai, T., Yu, C. Liang, X. Ouyang, X. Lu, H. Li, Tong, Y. 2013. Improving the photoelectrochemical and photocatalytic performance of CdO nanorods with CdS decoration, *CrystEngComm*, 15 4212-4216.
- Pan, Z., Dai, W. Z. R., Wang, Z. L. 2001. Nanobelts of Semiconducting Oxides, 9 947-1949.
- Pushpanathan, K., Sathya, S., Jaychithra, M., Gowthami, S. Santhi, R. 2012. Influence of reaction temperature on crystal structure and band gap of ZnO nanoparticles. *Mater. Manuf. Process.* 27, 1334–1342
- Pushpanathan, K., Vallalperuman, K., Seenithurai, S., Kodipandyan, R. and Mahendran, M. 2011. *Modern Physics Letters B*, Vol. 25, No. 18 1577–1589
- Rajkumar, N., Susila, V.M. K. 2011. Ramachandran On the possibility of ferromagnetism in CdO, Mn at room temperature. *J. Exp. Nanosci.* 6, 389.
- Reyesa, D. A., Delgado, G. T., Pérez, R. C., Marina, J. M., Ángel, O. Z. 2012. *Journal of Photochemistry and Photobiology A, Chemistry*, 228 22–27.
- Selvam, N. C. S., Kumar, R. T., Yogeenth, K., John Kennedy, L., Sekaran, G., Judith Vijaya, J. 2011. *Powder Technology* 211 250–255.
- Sravani, C. Ramakrishna Reddy, K.T., Jayarama Reddy, P. 1993. Influence of oxygen partial pressure on the physical behaviour of CdO films prepared by activated reactive evaporation, *Mater. Lett.* 15, 356-358.
- Srinivasaraghavana, R., Chandiramoulib, R., Jeyaprakashb, B.G., Seshadr, S. 2013. Quantum chemical studies on CdO nanoclusters stability, *Spectrochimica Acta Part A, Molecular and Biomolecular Spectroscopy*, 102 242–249.
- Tadjarodi, A., Imani, M. 2011. Synthesis and characterization of CdO nanocrystalline structure by mechanochemical method, *Materials Letters* 65 1025–1027.
- Tadjarodi, A., Imani, M., Kerdari, H., Bijanzad, K., Khaledi, D., Rad, M. 2014. Preparation of CdO Rhombus-like Nanostructure and Its Photocatalytic Degradation of Azo Dyes from Aqueous Solution, *Nanomaterials and Nanotechnology*, 4 1-10.
- Tadjarodi, A., Imani, M., Kerdari, H., Bijanzad, K., Khaledi, D., Rad, M. 2014. Preparation of CdO Rhombus-like Nanostructure and Its Photocatalytic Degradation of Azo Dyes from Aqueous Solution, *Nanomaterials and Nanotechnology*, 4:16, DOI: 10.5772/58464.
- Vijaykarthik, D. D., Kirithika, M., Prithivikumaran, N., Jeyakumaran, N. 2014. Synthesis and characterization of Cadmium Oxide nanoparticles for antimicrobial activity, *Int. J.Nano. Dimens.* 5 557-562.
- Waghulade, R.B., Patil, P.P. 2007. Renu Pasricha, *Talanta*, 72, 594.
- Yufanyi, D.M., Tendo, J.F., Ondoh, A. M., Mbadcam, J. K. 2014. *Journal of Materials Science Research*, 31-14.

\*\*\*\*\*